Concentric-Tube Airlift Reactors: Effects of Geometrical Design on Performance

J. C. Merchuk
Dept. of Chemical Engineering & Program of Biotechnology,
Ben Gurion University of the Negev, Beer Sheva 84105, Israel

N. Ladwa, A. Cameron, M. Bulmer, and A. Pickett
Porton Products Ltd., CAMR Porton Down, Wiltshire, England

Pressure drops, gas holdup, and mass-transfer coefficients were measured in two concentric-tube airlift reactors of 30 and 300 L (nominal volume). The aspect ratio and the ratio of riser to downcomer cross section were the same for both reactors, but the geometry of the gas separation section was different. The influence of the bottom and top clearances was studied using water and carboxymethyl cellulose solutions and covering a range of effective viscosity from 10^{-3} to 25×10^{-3} Pa·s. The pressure drop results expressed as a Euler number were satisfactorily correlated with Fr, Ga, and a bubble disengagement group M. Correlations are presented also for the gas holdup in the riser, downcomer, and gas separator. The last-mentioned coincides with the correlation for the total holdup in the reactor. The gas-liquid mass-transfer coefficients for all the liquids and geometric variables in both reactors were successfully correlated as Sherwood numbers.

Introduction

Airlift reactors (ALRs) have attracted the attention of researchers and industry due to their unique hydrodynamic characteristics, which make them more suitable than conventional systems for many processes (Siegel et al., 1988). However, in spite of important advances made in recent years toward understanding their behavior, for proper design and scaleup of these reactors a number of points have to be clarified.

The design of an ALR for a given range of operation variables implies the selection of a set of geometrical parameters. Published work on this subject has generally focused on the effect of the ratio of the cross-sectional area of a riser to that of a downcomer (Weiland, 1984; Chisti and Moo Young, 1987; Bello, 1981; Popovic and Robinson, 1988). Recently, Joshi et al. (1990) analyzed their model for external loop airlift, taking the slenderness ratio as a parameter. The height of the reactor has been considered in a previous model (Merchuk et al., 1992). The influence of the design of the gas-separation section at the top of the reactor was studied for gas-liquid (Siegel et al., 1986; Siegel and Merchuk, 1987) and gas-solid-liquid systems (Siegel et al., 1988). The influence of the design of the bottom section on the performance of the reactor had previously been recognized (Blenke, 1979).

All the above stress the importance of geometry in the scaleup of ALRs. The principal changes encountered when passing from laboratory to a larger scale are in the fluid dynamics of the system. Therefore, one of the most important factors in the design and scaleup of reactors is the influence of the geometry of the system on the flow of different phases present.

In the case of concentric-tube ALRs, the distance from the reactor base to the draft tube (bottom clearance) and the distance from the top of the draft tube to the top of the liquid level (top clearance) have received only minimal attention (Hwang and Fan, 1986; Sukan and Vardar-Sukan, 1987; Koide et al., 1984, 1988; Deng and Li, 1986).

The above results have the drawback of having been obtained on small vessels, where the ratio of wall surface area to volume is much higher than in a pilot- or industrial-size reactor. The relative influence of the frictional forces on the walls differs at different scales. In addition, liquid velocity will be much higher in taller equipment, as predicted by all available models (Merchuk et al., 1980; Merchuk and Stein, 1981; Chakravarty et al., 1974; Verlaan et al., 1986; Lee et al., 1987; Chisti et

Correspondence concerning this article should be addressed to J. C. Merchuk.
Present addresses of: A. Cameron, Southbank University, London; M. Bulmer, University College, London.

Table 1. Dimensions of the ALR Used (See Figure 1)

Nominal Vol. (L)	D (m)	D_{dr} (m)	D_s (m)	L (m)	L_{ar} (m)	C_B (m)	C_T (m)
30	0.158	0.110	0.213	2.00	1.395	0.012	0.170
"	"	"	"	"	"	"	0.308
"	"	"	"	"		0.020	0.170
"	"	"	"	"	"	"	0.308
300	0.318	0.216	0.318	4.10	3.27	0.010	0.040
"	"	"	"	"	"	"	0.240
"	"	"	"	"		0.020	0.040
"	"	"	"	"	"	"	0.240
"	"	"	"	"		0.040	0.040
"	"	"	"	"	"	"	0.240
"	"	"	"	"		0.080	0.040
"	"	"	"	"	"	"	0.240

al., 1988; Garcia Calvo, 1989). In addition, the range of variation of the clearances was rather narrow, and all liquids used in the experiments were Newtonian. It follows from the above that further studies are needed to clarify the effect of clearances on the hydrodynamic behavior of airlift reactors, especially in larger volumes.

In ALRs, the geometric characteristics of the reactor and the viscosity define the pressure drop in the circulation loop. The balance between this pressure drop and the hydrostatic pressure driving force (gas holdup) determines the liquid velocity, which in turn affects gas holdup. Indeed, all theoretical models and methods for calculating liquid velocity require a knowledge of the pressure drop in the different sections of the reactor or of the friction factors in these sections (Merchuk, 1990).

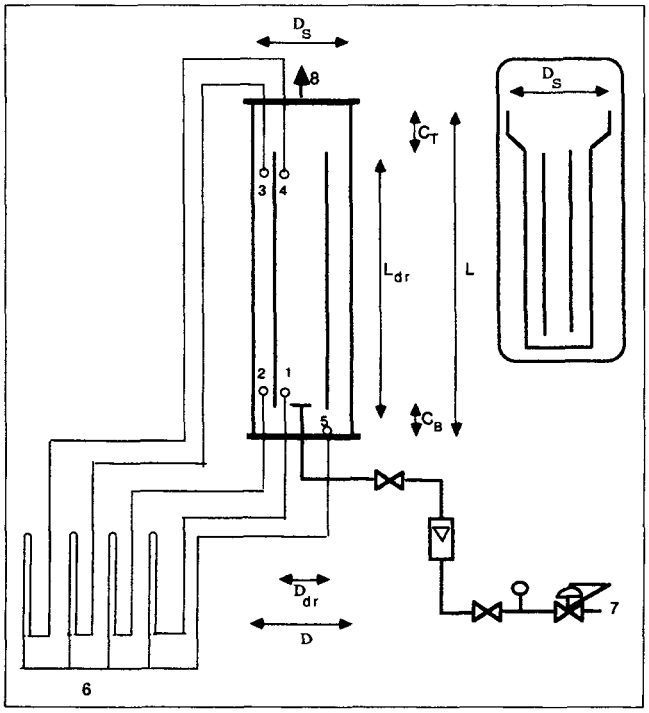

Figure 1. Experimental setup for the 300-L reactor.

1,2,3,4 = pressure probe positions; 5 = reference pressure probe; 6 = pressure measurement arrangement; 7 = process air inlet; 8 = exhaust air outlet; see dimensions in Table 1.

The pressure drop in the riser and downcomer can be evaluated using classical methods for two-phase pressure drop calculations (Lockhart and Martinelli, 1949; Oshinowo and Charles, 1974). A pressure drop correlation obtained specifically in an airlift reactor has recently been presented by Akita et al. (1988). However, the pressure drop at the bottom and at the top of the reactor, where a 180° deflection of the fluid creates complicated flow patterns, remains difficult to assess.

In this work, the results of a series of experiments in a 30-L and a 300-L (nominal volumes) ALR are presented. The effects of the geometrical characteristics of the system (such as bottom and top clearances, and gas separator shape) were studied. The measurements reported include pressure drop (correlated as *Eu* number), gas holdup in the riser, downcomer and gas separator, and gas-liquid mass-transfer coefficient (correlated as *Sh* number).

Experimental Methods and Apparatus

The two ALRs used had nominal volumes of 30 and 300 L, as shown in Table 1. Both were constructed from borosilicate gas columns. Bottom and top plates, as well as draft tubes, were metallic, and no deflection or deformation was observed during operation. The 30-L ALR was a commercially available fermenter (LH 4000, L.H. Fermentation, Slough, England) with a bottom plate modified to accommodate the sensors used in this work. The draft tube was made of stainless steel and served as gas sparger and heat exchanger. It was suspended from the top plates by three 0.0062-m-dia. tubes, which served as gas inlet line, and inlet and outlet for the heat exchanger fluid, respectively. The bottom clearance could be modified by using the bolts that secured the three tubes to the top plate. The draft tube diameter in Table 1 represents the mean between the internal and external measurements. The draft tube in the 300-L ALR was made of 16-gauge aluminum and was supported by three adjustable legs attached to the stainless-steel base plate. The legs covered less than 2% of the area available between draft tube and bottom, and their resistance to flow was neglected.

The gas separation section in the 30-L ALR had a larger diameter than the rest of the column, while in the 300-L ALR the section of the external tube did not change along the axis. The experimental setup in Figure 1 shows the shape of the gas separator of the 30-L ALR in the box.

The ring sparger was fixed 0.1 m from the base plate, and its diameter was 0.178 m. It was constructed from 0.0062-m-dia. stainless-steel-pipe, with 40-holes drilled in the top of the ring, each of 0.001-m-dia., equidistantly spaced around the circumference. This arrangement, while satisfactory in general, did not quite meet the requirements for satisfactory gas distribution over all the orifices of the sparger at the lowest gas flow rates. For the latter, the requirement that the Weber number based on the orifice diameter be greater than 2

$$We_o = (V_o^2 D_o \rho_o / \sigma) > 2 \qquad (1)$$

was not satisfied. This was a consequence of the wide range of flow rates used (a 27-fold change). Nevertheless, due to the small diameter of the orifices, no weeping was observed even when some of the orifices were not active.

Pressure drop and holdup measurements

As shown in Figure 1, the stainless-steel base of the 300-L reactor had three ports for pressure probes and the top plate had two ports for pressure sensors. The probes were located symmetrically on either side of the draft tube (the riser and downcomer sections). In the 300-L ALR, the measurement of pressure differences between pairs of sensors was performed indirectly, as the pressure at each individual point was measured with reference to a single common point, namely, an additional reference pressure sensor located in the base plate of the reactor (point 5 in Figure 1). All the sensors were connected to the reference via inverted manometers. Air bubbles in the manometer lines were removed by frequent bleeding of the system; pressure oscillations were dampened out by the insertion of capillary sections in the lines. The setup for pressure drop measurements in the 30-L ALR was similar to that in the 300-L ALR.

In the measurement of pressure drop, the location of the measuring probes is of some importance. When a pressure measurement is carried out in a pipe, special care is taken to ensure that the flow is completely developed at the measuring point. When this is not possible, as in flow measurement by orifice devices, the point where the pressure tap is located becomes very important. Perry (1963) indicates the importance of ensuring that the measurement corresponds to the static head, with no interference from the dynamics of the fluid.

Most of the experimental devices used for research into airlift reactors are relatively small. To obtain a satisfactory measurement of the pressure drop, the latter must be measured over the whole or the greater part of the height of the device. This usually means that the location of one or more measuring points must be at the bottom and at the top of the tubes. The fluid flow in these zones is complicated and difficult to describe due to the 180° turns of the gas-liquid mixture, changes in the cross-sectional area, and stagnant zones. These effects have been qualitatively described (Blenke, 1979; Merchuk, 1986; Thomas and Janes, 1986). It follows that the pressure drop data used in gas holdup calculations in airlift reactors may be distorted due to incorrect location of the pressure taps. Since determining the correct points for measuring the pressure in ALRs was one of the aims of this work, the position of the pressure probes was made both axially and radially adjustable.

Since the distance between the bottom of the draft tube and the base of the reactor, as well as the liquid height above the top of the draft tube, was varied during the experiments, the liquid volume within the reactor changed depending on the conditions, from 258 to 280 L in the larger ALR and from 26 to 31 L in the smaller one.

The liquids used were dimineralized water and solutions of CMC (Sigma sodium salt, Medium Viscosity, No. C-4888), approximately 0.5 and 0.25 wt. % in the same water. The rheology of the solutions was evaluated with a Physica Viscolab LC1 rotational viscometer. The constants K and n in the power law

$$\tau = K\gamma^n \tag{2}$$

were obtained by regression of the viscometer results, Table 2. The range of shear rate used was $35\ s^{-1} < \gamma < 4{,}030\ s^{-1}$. Each CMC solution batch was used for two or three days. Sodium azide 0.1% was added as growth inhibitor. The rheological measurements were checked twice a day to assure that viscosity had not been reduced by biodegradation.

Air was used as the gas phase. Flow rates were measured with calibrated rotameters. Since one of the most likely fields of application of ALR is in the culture of plant and animal cells, where air requirement is usually low, the range of superficial velocity used was varied from 1.7×10^{-3} to 4.4×10^{-2} m/s in the 30-L ALR and from 1×10^{-3} to 2.6×10^{-2} m/s in the 300-L ALR.

The gas holdup in the riser and the downcomer was calculated from the measured pressure drop along the corresponding section using the expression:

$$\phi_{r,d} = 1 - (\Delta P_{r,d}/\rho_L g \Delta z) \tag{3}$$

where the subscripts indicate that the above can be applied either to the riser or to the downcomer.

The total holdup was calculated from the measured ungassed liquid and dispersion height:

$$\phi_T = (H_d - H)/H_d \tag{4}$$

The gas holdup in the gas separator was calculated from a gas volume balance:

$$\phi_T V_T = \phi_r V_r + \phi_d V_d + \phi_s V_s + \phi_b V_b \tag{5}$$

neglecting the last term in the righthand side in view of the small volume and very low gas holdup in that section. Taking into account the geometrical characteristics of the system, the separator holdup may then be found from:

$$\phi_s = \frac{\phi_T V_L/(1-\phi_T) - \phi_R L_{dr} A_{dr} - \phi_d L_{dr} A_a}{V_L/(1-\phi_T) - L_{dr}(A_{dr}+A_a) - C_b A} \tag{6}$$

Mass-transfer coefficient measurements

Three polarographic oxygen electrodes (Marubishi DY-2p) were used in the 300-L ALR. One was housed in the base plate, and the other two were inserted through the top plate, down to the upper part of the riser and of the downcomer zone, respectively. In the 30-L ALR, only two electrodes were installed: one flush with the bottom plate beneath the draft tube wall and the other in the gas separation zone. For the latter, the socket orginally provided in the conical part of the column (Figure 1) was utilized.

The electrode readings were collected with a Labpack data acquisition system, at a sampling frequency which varied from 0.05 sample per second for the lowest mass-transfer rates, to 10 samples per second at the highest mass-transfer rates. The three electrodes (or two, in the 30-L ALR) were sampled simultaneously.

The dynamic method was used for the measurements. The reactor was gased with N_2 until the oxygen meter readings indicated that all of the oxygen had been displaced, whereupon the gas flow was changed to air by turning a three-way valve. The N_2 flow rate was set to the desired air-flow rate before the start of the run to ensure continuity of the fluid dynamics of the system. For the 0.5% CMC solutions the switch from

N_2 to air was not instantaneous. A period of 30 s was allowed before starting the air flow to allow for the lower free rise velocity and lower coalescence of bubbles in this liquid. This enabled the disengagement of most of the nitrogen bubbles. The longer time required to reach saturation (smaller k_La) justified neglecting the effect of the 30-s delay in the calculations.

The temperature of the liquid inside the reactor was measured with a standard thermometer. Temperature values were between 16 and 21°C. All values of the mass-transfer coefficient obtained were corrected for temperature, as explained in the next section.

The mass-transfer coefficient k_La was calculated from the recorded curves of O_2 concentration vs. time using Eq. 7, which assumes a first-order response of the dissolved oxygen probe (Weiland and Onken, 1981):

$$\frac{C_e - C_{eo}}{C^* - C_{eo}} = 1 - \left\{ \frac{m}{(1-m)} \left[\exp\left(\frac{-t}{T_e}\right) - \exp\left(-\frac{mt}{T_e}\right) \right] \right\} \quad (7)$$

with m given by:

$$m = (k_L a\, T_e)/(1 - \phi_T) \quad (8)$$

The volumetric mass-transfer coefficient was obtained by fitting Eq. 7 to the experimental curve of concentration vs. time. The optimal value of m was used to calculate k_La from Eq. 8. The mass-transfer coefficient at 20°C was calculated following APHA (1981) from:

$$k_La(20) = k_La(T)(1.024)^{(20-T)} \quad (9)$$

where $k_La(20)$ and $k_La(T)$ are the mass-transfer coefficients at 20°C and at the experimental temperature, respectively. All the data presented here were converted to 20°C.

The time constants for the oxygen electrodes were obtained experimentally for each electrode. This was done by rapidly transferring the probe from a liquid into which N_2 was bubbled (zero oxygen concentration) to a liquid saturated with air, both vigorously stirred. The electrode response to the step change was recorded, and T_e obtained as the time for reaching 63.2% of the steady-state response. This procedure was repeated after each change of membrane in the probe. The values of T_e ranged from 3.2 to 5 s for the three electrodes in all the different liquids. The temperature of the liquid was the same as in the ALR in the corresponding run.

Experimental Results

A series of measurements were performed in the 300-L ALR for different positions of the pressure sensors in both the radial and the axial directions (Ladwa et al., 1988). As a result, it was decided that the optimal radial position in the downcomer was halfway between the external tube and the draft tube. For the riser, a radial position symmetrical with respect to the draft tube was selected. For a specific ALR used, this meant that the two sensors of a pair at the same axial position were 0.054 m apart, with the wall of the draft tube between them.

The optimal axial position at the top and bottom of the ALR was found to be 0.07 m below the upper rim of the draft tube and 0.075 m above the lower end of the draft tube, respectively.

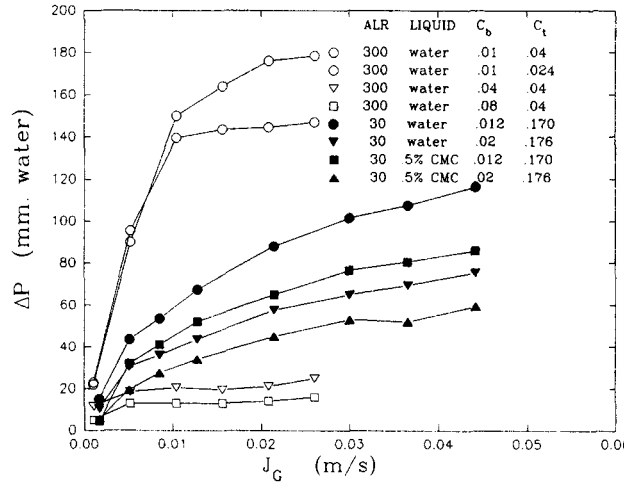

Figure 2. Pressure drop at the bottom of the ALRs tested as a function of the superficial velocity for bottom and top clearances, water and 0.5% CMC solution.

Pressure drop

Once the optimal position for the pressure sensors was established, it became possible to evaluate experimentally the influence of the draft tube clearance on the pressure drop. The experiments were run with water in both reactors. Measurements of total holdup and bottom pressure drop with CMC solutions were also carried out on the 30-L ALR.

Figure 2 presents some of the results for the dynamic pressure drop at the bottom of the ALRs tested. In general, the pressure drop increases at low gas superficial velocity J_G and then tends to a plateau where further increases of J_G do not have much influence on it. This phenomenon is especially pronounced in the 300-L ALR. It may be interpreted as due to a constant liquid velocity independent of J_G. This situation arises because the increase in J_G increases the riser gas holdup and liquid velocity is proportional to $(\phi_r - \phi_d)$ (V_L increases as well). However, any increase in V_L leads to enhancement of bubble entrainment into the downcomer, which increases ϕ_d, attenuating the increase in V_L. Eventually, this negative feedback process leads to a situation where the holdups of riser and downcomer increase in a similar way, the difference between them becoming independent of the superficial gas velocity.

When the free area for liquid flow between bottom plate and draft tube is very constrained, changes in the bottom clearance have strong influence on pressure drop. This is not so for clearances higher than 0.04 m. As shown in Figure 2, the data for $C_b = 0.08$ m are close to those corresponding to $C_b = 0.04$ m. For large bottom clearance, the influence of the gas superficial velocity is very small even at low J_G, and the top clearance does not affect the pressure drop.

Figure 2 also shows some of the pressure drop data measured in the 30-L ALR for two bottom clearances and two liquids: water and 0.5% CMC. The plateau observed in the 300-L ALR was not observed here. This is apparently related to the difference in gas separator configuration between the two reac-

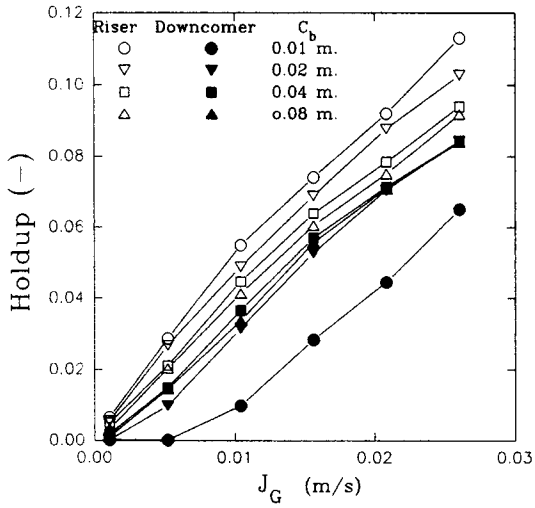

Figure 3. Riser and downcomer gas holdup in the 300-L ALR for bottom and top clearances of $C_T = 0.04$ m.

System: air-water.

tors. Because of the larger cross section in the gas separator, the 30-L ALR allowed better gas disengagement, and the phenomenon of negative feedback control of the liquid velocity was delayed until much higher J_G.

The influence of the bottom clearance C_b was also very important for all of the liquids used. In all cases, a bottom clearance of 0.012 m gives a much higher pressure drop than a bottom clearance of 0.02 m. It is interesting to note, however, that the highest pressure drop is obtained with pure water, and ΔP becomes smaller as the CMC concentration increases. This must be ascribed to a corresponding decrease of the liquid velocity due to the increase in effective viscosity. Since independent measurements of liquid velocity were carried out with water only, this inference cannot be corroborated.

Figure 2 also shows that the rheological properties of the liquid have a much stronger influence when C_b is smaller. Indeed, the curves for $C_b = 0.012$ m are much farther apart than those for $C_b = 0.02$ m.

The pressure losses in the 180° deflection at the top of the ALRs, which account for the pressure drop in the gas separation section, were also measured. The results showed that this pressure drop is much lower than at the bottom and in fact it is of the same order as the experimental error of the measurement.

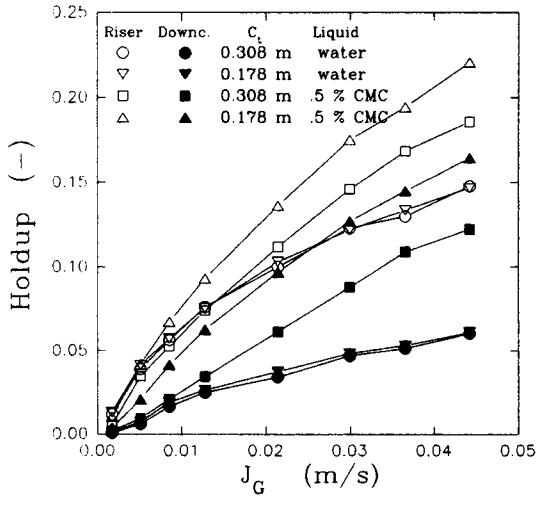

Figure 4. Riser and downcomer gas holdup in the 30-L ALR for top and bottom clearances of $C_b = 0.012$ m.

Gas holdup

Experimental measurements of gas holdup were performed in both ALRs using water and air. Experiments were also performed with 0.25% and 0.5% CMC solutions.

The effect of bottom clearance on riser and downcomer gas holdup are shown in Figure 3 for the 300-L ALR air-water system. The gas holdup increases in the riser as the bottom clearance decreases. This can be understood as caused by a decrease in the liquid velocity. This is especially evident in the data for the downcomer gas holdup, since for the smallest bottom clearance the velocity of the liquid is so restricted by the pressure drop in the bottom of the reactor that almost all of the gas disengages in the gas separator. The gas holdup in the downcomer is almost nil at low values of the superficial gas velocity J_G. In the 30-L ALR, where the influence of C_b on V_L was measured, the same trend was observed: V_L decreases as C_b decreases.

Figure 3 presents the data corresponding to a top clearance of 0.040 m. A set of experiments with $C_t = 0.024$ m (not shown) showed essentially the same behavior, with the exception of the data for $C_b = 0.01$ m. In the latter case, the holdups corresponding to $C_t = 0.240$ m were slightly lower.

Figure 4 shows the gas holdup in the riser and downcomer of the 30-L ALR, for a bottom clearance of $C_b = 0.012$ m and two values of the top clearance: $C_t = 0.178$ and $C_t = 0.308$ m. Data are presented for water and 0.5% CMC solution. While for water C_t has a small effect, this is not so for the more viscous solutions. In the latter, the lower rising velocity of the bubbles causes more of them to be entrained and carried down by the liquid, and therefore the larger residence time in the disengagement section due to the larger C_t is very important in determining the fraction of bubbles that recirculate. The lower C_t gives a shorter residence time in the separator, a larger bubble recirculation, and, therefore, a larger gas holdup. This is especially evident in the downcomer for the more viscous of the CMC solutions (0.5%).

Figure 5 displays the effects of both clearances on the riser holdup of the 30-L ALR for the 0.5% CMC solution. Even here, where as explained above the top clearance has its maximal effect, the bottom clearance is the leading parameter. The holdup for $C_b = 0.012$ m is almost twice of that corresponding to $C_b = 0.020$ m. As suggested earlier, this can be understood as the effect of the liquid velocity on the gas retention. Thus, the bottom clearance imposes strong restrictions on the flow of the move viscous 0.5% CMC solution.

The measured total holdup for both reactors is shown in Figure 6 as a function of the superficial gas velocity J_G for various values of the bottom clearance C_b. It is interesting to note that in the 300-L ALR, the total gas holdup is essentially the same for $C_b = 0.040$ and 0.080 m, indicating balancing of

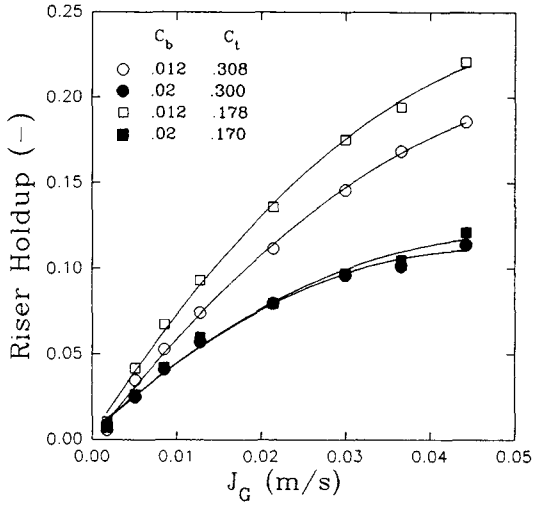

Figure 5. Riser gas holdup in the 30-L ALR for top and bottom clearances, for 0.5% CMC solution.

the decrease of ϕ_r by an increase of ϕ_d as C_b and thus the liquid velocity increase.

The total gas holdup for the lower bottom clearance, $C_b = 0.010$ m, is the lowest of the data for the 300-L ALR. This is due to the contribution of the downcomer, since the riser holdup for this situation, Figure 3, is the highest.

The balancing effects of riser and downcomer can also be seen in the total holdup obtained for the 30-L ALR. The total holdup was higher for the 0.25% and 0.5% CMC solutions than for water, especially at high J_G and for the 0.5% CMC solution. This is due to the lower bubble disengagement, which in turn results from the lower rising velocity in the more viscous liquids.

In general terms, the separator gas holdup behaves in the same manner as the total gas holdup. The effects of the different gas separator designs can be seen by comparing Figures 3 and 4. With the exception of the data for $C_b = 0.010$ m in

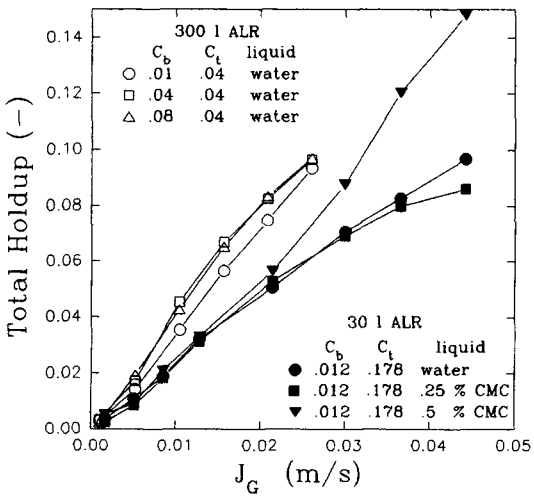

Figure 6. Total gas holdup in both ALRs for constant value of top and bottom clearances and two liquids.

the 300-L ALR (predominant bottom clearance control) and those for the 0.5% CMC solution in the 30-L ALR (predominant viscosity control via low bubble rising velocity), all the other data indicate that disengagement was much more effective in the 30-L ALR. This indicates that the cross-sectional area of the gas separator has a strong influence on the fluid dynamics of the reactor. This was clearly shown by the regression analysis, which is presented in the next sections.

Mass-transfer data

The use of Eq. 7 to calculate the mass-transfer coefficient k_La implies that there is perfect mixing of the liquid phase in the reactor. If this assumption were true, then measurements of the dissolved oxygen concentrations should be independent of the location of the probe, and every measurement should give the same results.

The response of the three D.O. electrodes after a step change of oxygen concentration in the gas inlet (from nitrogen to air) revealed cyclic patterns due to the circulation in the reactor. This shows that the ALR does not behave strictly like a perfectly mixed vessel. However, the question remains whether the use of Eq. 7 for k_La entails a large error of calculation or not. If the error is too large, a much more complicated method of calculation will have to be used (Merchuk et al., 1992). The problem of whether the ALR can be considered perfectly mixed has been addressed both theoretically (Andre et al., 1983) and experimentally (Siegel et al., 1990). The criterion that determines the applicability of the perfect mixing assumption in the determination of k_La is related to the characteristic time for mass transfer, divided by the circulation time. The required condition is:

$$(k_L a\, t_c) < 2 \tag{10}$$

An analysis of the data presented here shows that condition 10 is fulfilled in almost all the experimental runs. Therefore, even if a more sophisticated elaboration of the data could be carried out, the simplicity of the calculations by Eq. 7 appears to outweigh the improvement that could be obtained at the cost of much computational time by the more sophisticated method of Merchuk et al. (1992).

This point can be further explored by comparing the k_Las calculated from the outputs of each of the electrodes separately using Eq. 10. Figure 7 shows the k_Las obtained for a bottom clearance of 0.040 m and a top clearance of 0.040 m. The k_Las calculated for probes at the top of the riser and at the top of the downcomer are almost the same. The bottom probe (Eq. 3) gives a slightly lower value, especially at high superficial gas velocity, the maximum difference accounting to 20–25%.

Data for higher top clearance would show somewhat higher values of k_La, but with almost the same pattern. Similar figures can be obtained for all the other values of the bottom clearance. It was, therefore, decided to treat the data obtained from probe 1 (at the top of the riser), as representative of the mass transfer in the ALR.

Figure 8 shows the mass-transfer coefficient as a function of the bottom clearance for a series of superficial gas velocities. The top clearance was 0.040 m. The general pattern for the higher gas superficial velocity is a slight decrease in mass-transfer rate as bottom clearance increases. For $J_G = 0.001$

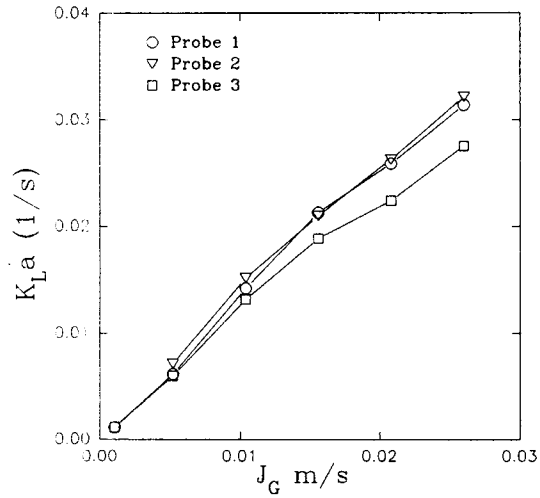

Figure 7. Mass-transfer coefficient $k_L a$ in the 300-L ALR, calculated from the response of probes at different locations.

Probe 1 = top of the riser; probe 2 = top of the downcomer; probe 3 = bottom of the downcomer; system, air-water.

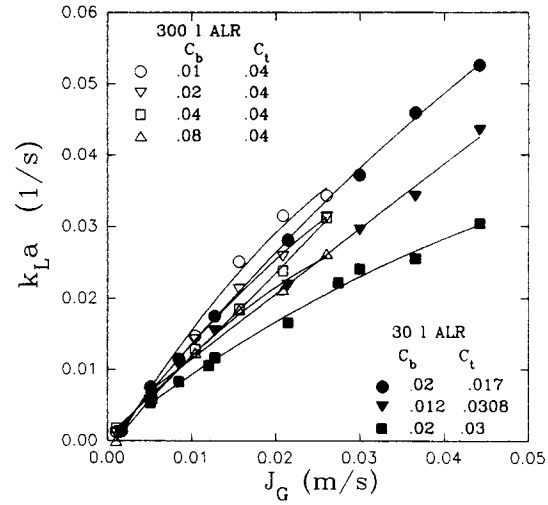

Figure 9. Mass-transfer coefficient $k_L a$ in both ALRs, as a function of gas superficial velocity, for water, showing the effect of bottom and top clearances.

m/s and 0.0052 m/s, the mass-transfer coefficient is practically independent of C_b. This is to be expected since at very low gas superficial velocities the gas holdup is very small, and as a result the liquid velocity is so low that the constriction at the bottom does not affect the holdup at all.

Figure 9 shows some of the calculated values of the mass-transfer coefficient for water in both reactors. The mass-transfer coefficient is higher for the lowest C_b. This is parallel to the behavior of the riser holdup as noted earlier. The effect of the bottom and top clearances for the 30-L ALR are clearly seen in the figure. The highest value of $k_L a$ is obtained for the lowest values of both C_t and C_b. Once again, this observation concurs with the data on the riser gas holdup. The effect observed on $k_L a$ is substantially stronger than the one observed on the total gas holdup (Figure 6). This can be understood considering the role of the liquid velocity. When C_t and C_b lead to a higher V_L, more bubbles are entrained. But, since the size of the entrained bubbles is smaller than the mean bubble size, $k_L a$ increases more rapidly than the holdup due to the larger interfacial area.

The mass-transfer coefficient for the two CMC solutions used in the 30-L ALR is presented in Figure 10. Both clearances have a negligible effect on $k_L a$ for the 0.25% CMC solution. The more viscous 0.5% CMC solution gives lower $k_L a$ values, contrary to the higher gas holdup seen above. The reason for this may well be a larger bubble size due to the increase in

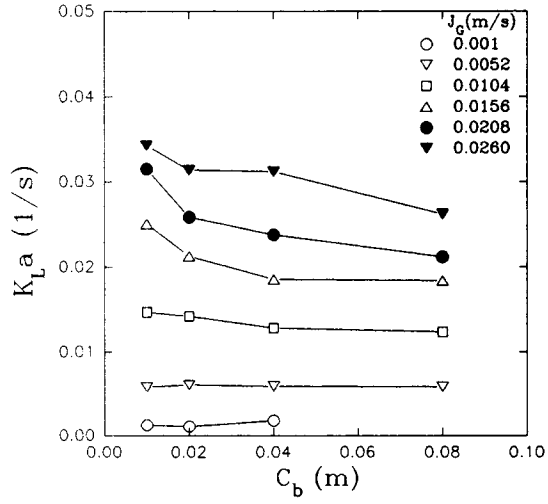

Figure 8. Mass-transfer coefficient $k_L a$ in the 300-L ALR, as a function of bottom clearance, for a constant top clearance of 0.04 m and various values of gas superficial velocity, J_G.

System: air-water.

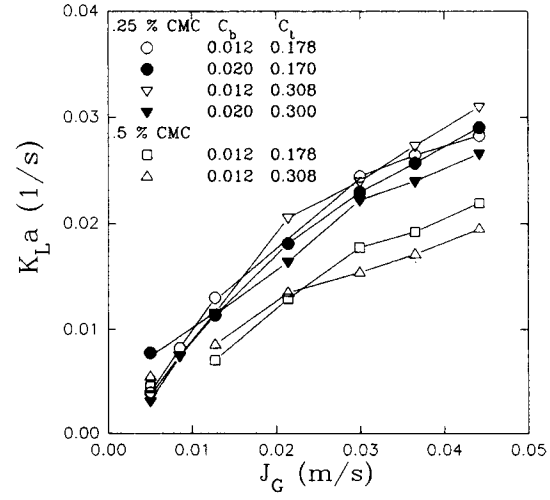

Figure 10. Mass-transfer coefficient vs. gas superficial velocity in the 30-L ALR, for viscous solutions, showing the effects of bottom and top clearances.

Table 2. Rheological Properties of the CMC Solutions at 25°C

Solution	K (Pa·s^n)	n
0.25 % w/v	0.016	0.902
0.5 % w/v	0.035	0.864

viscosity. In this case, the effect of the top clearance is perceptible; once again, the higher C_t, the lower k_La.

The correlation of the experimental values of k_La for both scales of ALRs and the range of geometrical characteristics and physicochemical properties tested is presented in the next section.

Correlation of the Experimental Results

Pressure drop

Since the two reactors utilized differ in scale, but not in the tube diameter ratio R or in the slenderness S, these variables can be ignored in our case. The length that represents the horizontal distance traveled by a recirculating bubble from the top of the riser to the top of the downcomer was considered as one of the geometrical variables. In the case of concentric cylinders, this length is independent of the draft tube diameter and equals half of the radius of the separator.

The surface tension is not considered, because it remained practically constant for all the liquids used. Neither liquid velocity nor the gas holdup is considered, since these are not independent variables, and they are not usually known *a priori*. The gas density was considered negligible, compared with the density of the liquid, and the effective viscosity was based on the relation proposed by Nishikawa et al. (1977):

$$\mu_{\text{eff}} = K(5{,}000 \cdot J_G)^{n-1} \tag{11}$$

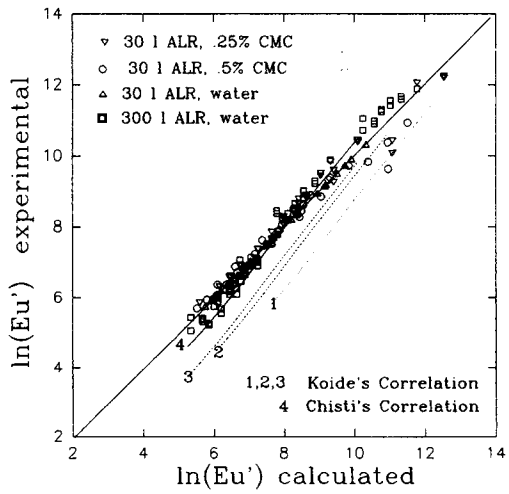

Figure 11. Experimental vs. calculated Euler number in both ALRs and various liquids and bottom clearances, as predicted by Eq. 19 and compared with previously published correlations.

1 = Euler number predicted using the correlation by Koide et al. (1984); 300-L ALR, for $C_b = 0.01$ m; 2 = Ibid., $C_b = 0.04$ m; 3 = Ibid., $C_b = 0.08$ m; 4 = Euler number predicted using the correlation by Chisti et al. (1988), 300-L ALR, for $C_b = 0.01$ m.

where K and n are the consistency and flow behavior indexes, given in Table 2.

The disengagement ratio defined by Siegel and Merchuk (1991):

$$DR \propto \frac{\text{Time for Gas Disengagement}}{\text{Time of Horizontal Flow in the Separator}} \tag{12}$$

which proved to be a useful correlator for systems of different geometries, reduces in the case of concentric cylinders to:

$$DR = (D/D_S)[(R^2 - 1)/R] \tag{13}$$

Since R is practically the same for both systems, this group is equivalent to the bubble separation group which we obtained from the dimensional analysis:

$$M = D_s/4D \tag{14}$$

which represents the mean horizontal path of a recirculating bubble, relative to the external diameter.

An analysis of the 182 experimental data showed that a satisfactory correlation ($r^2 = 0.966$) was obtained as:

$$Eu' = 0.858\, Fr^{-1.51}\, Ga^{0.06}\, X_{dr}^{-1.1}\, M^{4.2} \tag{15}$$

which is based on data within the following range:

$$\begin{gathered} 6\times10^{-4} < Fr < 350\times10^{-4} \\ 3\times10^{7} < Ga < 6\times10^{11} \\ 0.04 < X_{dr} < 0.4 \\ 0.22 < M < 0.34 \end{gathered} \tag{16}$$

Since in the Euler number the superficial gas velocity appears with the exponent -2, the correlation shows that the pressure drop depends on J_G with an exponent of approximately 1/2. The exponent of the Galileo number shows a small positive effect of viscosity on the pressure drop which, within the range given in the inequalities (Eq. 16), would lead to a maximal increase of 20% in the pressure drop. On the other hand, the bottom clearance has a strong influence on ΔP, and the present correlation predicts that it can lead to an increase in the pressure drop by a factor of 14, within the range of C_b studied. The bubble separation group M defined here has a strong influence on the pressure drop, due to its influence on the liquid velocity.

Figure 11 shows the predictions of Eq. 15 vs. the experimental data within the range of variables in Eq. 16. It can be concluded that the correlation found is satisfactory for the prediction of pressure drop in concentric tube airlift reactors over a wide range of physicochemical, geometrical and operational variables.

In Figure 11, data calculated from the correlation by Koide et al. (1988), for values of the variables corresponding to the 300-L ALR with C_b of 0.01, 0.04, and 0.08 m, are presented in lines 1, 2, and 3, respectively. The lines become closer to Eq. 19 as C_b increases. This is to be expected, since Koide's correlation is based on data obtained with relatively high values

of C_b. It should be remembered that, as seen in Figure 2, C_b has its strongest influence on ΔP when its value is low.

Line 4 in Figure 11 was calculated from the expression by Chisti et al. (1988), also simulating the 300-L ALR, with $C_b = 0.08$ m. The values are almost coincident. Chisti's correlation would predict a slightly stronger dependence of pressure drop on Eu' as compared with our correlation. For lower values of C_b, Chisti's correlation underestimates the pressure drop, similar to Koide's.

Both Chisti's and Koide's correlations require a knowledge of the liquid velocity and gas holdup, which are not known *a priori* and are not easily measured. The present correlation, on the other hand, is based on data obtained in pilot-scale reactors and requires only a knowledge of the geometrical characteristics of the equipment, the liquid properties, and the gas inlet rate, which is the manipulated variable in airlift reactors. All of them, in addition to the satisfactory fit of 182 data, covering a wide range of gas flow rates, reactor dimensions, and liquid properties, lend Eq. 15 a wider range of applicability. It should be remembered that surface tension, R and S, were not varied in the reported experiments. Nevertheless, its comparison with previously published correlations indicates that Eq. 15 is quite general. However, the correlation should be validated by independent experiments, since the effect of surface tension has still to be investigated.

Gas holdup

Correlations were obtained for ϕ_r, ϕ_d, ϕ_T, and ϕ_s on the basis of 180 experimental data in each case. The range within which these correlations are valid is given in inequalities (Eq. 16).

The correlations for each of the partial gas holdups were:

$$\phi_r = 1.5\,Fr^{0.87} M^{-0.4} X_{dr}^{-0.19} Y^{-0.2}, \quad r^2 = 0.968 \qquad (17)$$

$$\phi_d = 4.76\,Fr^{1.3} X_{dr}^{0.65} M^{-3.8} Ga^{-0.09}, \quad r^2 = 0.85 \qquad (18)$$

$$\phi_T = 0.29\,Fr^{1.05} M^{-2.5} X_{dr}^{0.1} Y^{-0.07}, \quad r^2 = 0.974 \qquad (19)$$

The last expression is valid also for ϕ_s. A parity plot for the correlation of ϕ_r, Eq. 17, is shown in Figure 12.

Correlations 17–19 reveal the roles played by the different regions in the ALR. The relative contributions of riser and downcomer to the total holdup are different and complementary. The main variable is the Fr number, which represents here the influence of gas input rate (and also energy input rate). It affects the holdup much more strongly in the downcomer than in the riser, and the balance between them gives an exponent of almost 1 (1.05) for the total holdup. It is interesting to note that the behavior of the holdup in the gas separator is very close to that of the total holdup. The bottom clearance, represented by the ratio X_{dr}, exerts its influence on the gas holdup in all the regions. The exponent of X_{dr} is negative in the correlation of holdup in the riser, indicating that as C_b increases ϕ_r decreases. As mentioned above, this can be seen as the effect of the flow restriction in the liquid velocity. In the downcomer, however, the exponent is positive and quite large, indicating the effect of the liquid velocity. As C_b increases, the liquid circulation increases as well, and more gas

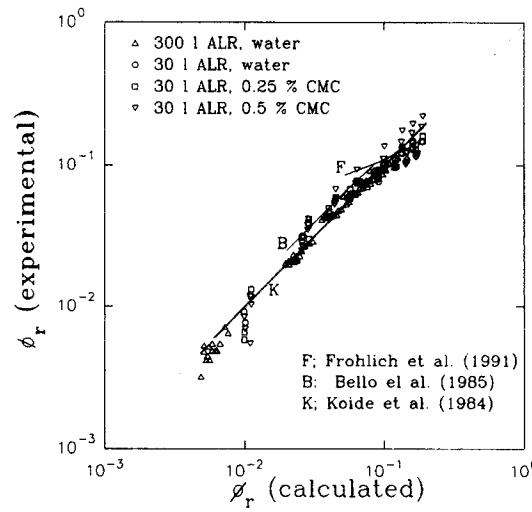

Figure 12. Parity plot of experimentally obtained values of the riser holdup vs. those calculated from Eq. 23 and comparison with data and correlations previously published.

bubbles are carried over into the downcomer. The exponent 0.65 on X_{dr} in Eq. 18 indicates that ϕ_d could be increased up to fourfold by changing the bottom clearance within the range of variables tested here.

The effect of the top clearance, represented by the ratio Y, had a modest influence on the riser and the total holdups, but none on the downcomer holdup. An increase in the top clearance diminishes the gas holdup, as indicated by the negative exponent. The correlations show that the viscosity, at least for the liquids tested and within the range of the variables inspected, does not have a statistically significant influence on either total holdup or riser holdup. It does significantly affect the downcomer holdup, because of the strong influence of the free rising velocity of the bubbles on the bubble entrainment. This influence is not detected in the overall holdup, because the holdup in the downcomer is smaller than in the other regions of the reactor and its contribution is relatively small. In consequence, the Ga number does not show a statistically significant influence on the total holdup. It should be noted, however, that at the higher values of J_G and the highest CMC concentrations, a considerably higher ϕ_T is observed (Figure 6). This does not have much of an effect on r^2, but it must be noted that the correlation may underestimate the effect of viscosity under the above conditions.

In spite of the limitations mentioned already (constant R and S and surface tension in the database), correlation 17 seems to give satisfactory results when compared with the literature. Figure 12 shows a line representing data reported by Koide et al. (1984). This correlation fits those data satisfactorily. The data by Fröhlich et al. (1991) are also well represented by Eq. 17. In addition to these experimental data, Figure 12 also shows the correlation by Bello et al. (1985). This correlation is very close to that presented here. It should be taken into account that Bello's correlation requires the liquid velocity as an argument. In our case, we took the velocity corresponding to the largest value of C_b, which is closer to the range of variables taken by Bello et al. (1985).

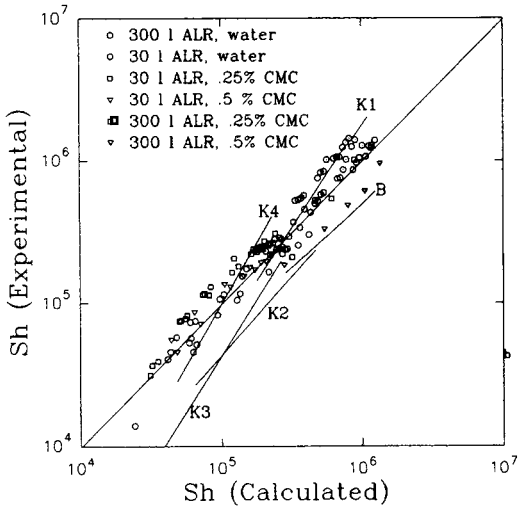

Figure 13. Parity plot of experimentally obtained values of the mass-transfer coefficient in both ALRs presented as *Sh* vs. those calculated from Eq. 28.

The lines represent predicted using other correlations: B-Bello et al. (1985), 300-L ALR, water, $C_b = 0.08$ m, $C_T = 0.24$ m; K1-Koide et al. (1983), 300-L ALR, water, $C_b = 0.08$ m, $C_T = 0.24$ m; K2-Koide et al. (1983), 30-L ALR, water, $C_b = 0.02$, $C_T = 0.170$ m; K3-Koide et al. (1983), 30-L ALR, 0.25% CMC, $C_b = 0.012$ m, $C_T = 0.178$ m; K4-Koide et al. (1983), 30-L ALR, 0.5% CMC, $C_b = 0.012$ m, $C_T = 0.178$.

Mass-transfer coefficients

The correlation was based on 128 data, each representing the average of a duplicated experiment. The set included k_La obtained with both water and CMC solutions in the 30-L ALR and with water in the 300-L ALR.

The ranges of the variables are the same as indicated before. The best fit was obtained with the following expression:

$$Sh = 17.3 \times 10^3 Fr^{0.9} M^{-3.4} Ga^{0.13} X_{dr}^{-0.07} Y^{-0.18} \qquad (20)$$

The correlation for the Sherwood number (Eq. 20) shows an exponent of 0.9 on *Fr*, which is close to results of Siegel and Merchuk (1991). The influence of apparent viscosity, represented by the Galileo number, reflects the decrease in mass-transfer rate expected from an increase in viscosity. The exponent 0.13, applied to the range of variations of *Ga*, would give a decrease of around 70% for the maximal viscosity in the range tested. The exponent of the effective viscosity is -0.26, smaller than the exponent -0.89 found by Popovic and Robinson (1989) in an external-loop ALR and in complete coincidence with the -0.25 exponent proposed by Umeno et al. (1991).

Considering that diffusivity is almost unaffected by the changes in viscosity in the case of large polymers like CMC and that the density did not change much, the Sherwood number in Eq. 20 is strictly a dimensionless form of the mass-transfer coefficient, and the correlation is not expected to take into account changes in ρ or D_L. Here, we have chosen to concentrate on the effect of other variables. The three geometrical factors considered here are the bottom and top clearances, and the bubble disengagement group. Both clearances affect the mass-transfer rate in modest proportions. Considering that the range of variation of X_{dr} is one order of magnitude, the correlation provides a maximal decrease of $10^{-0.07}$, approximately 15%. The same analysis gives a maximal change of around 30% due to the top clearance variation *Y*. The influence ascribed to the bubble disengagement group, *M*, has a maximal influence of up to 70%, obviously the most important of the three.

A comparison between Eq. 20 and the experimental results is shown in Figure 13. In addition to the experimental data obtained on both ALRs with the three liquids used, the results predicted by correlations available in the literature are shown for comparison. The line labeled B was obtained from the correlation by Bello et al. (1985) for the values of the parameters corresponding to the 300-L ALR with a bottom clearance of 0.08 m. The line runs at 45°, but underestimates the mass-transfer rate. The correlation by Koide et al. (1983) was used to simulate both the ALRs, with water and CMC solutions. This correlation tends to overestimate the mass-transfer rate at high *Sh* and underestimates it at low *Sh*. In the range of the experimental values, however, it gives results quite close to the correlation presented in this article. In these calculations, only the largest values of C_b were taken. Koide's correlation would not be a good predictor for low values of C_b, since it was obtained from data where the bottom clearance was not very small.

McManamey and Wase (1986) found a parallel behavior of total holdup and mass-transfer coefficient in an external-loop ALR. The correlations obtained in this work indicate that gas holdup in the riser is the variable that behaves most nearly similar to the mass-transfer coefficient. This difference may be due to the negligible downcomer gas holdup in the experiments considered by the above authors.

Conclusions

The experimental results on dynamic pressure drop for two concentric airlift reactors differing in volume by one order of magnitude, for several bottom clearances and for liquids of effective viscosity ranging from 0.001 to 0.025 Pa·s, were successfully correlated as a modified Euler number. The geometric characteristics of the reactor do exert an important influence on the dynamic pressure drop. The most important of these characteristics is the bottom clearance.

The experimental results for the holdup and mass-transfer coefficients were successfully correlated using expressions obtained via dimensional analysis. Correlations for the gas holdup are presented for each of the different hydrodynamic regions in the ALR: riser, downcomer, and gas separator. The last one showed almost complete coincidence with the total holdup. The bottom clearance was found to be a parameter of importance for prediction of both riser and downcomer holdups, as was the bubble separation group, *M*.

The mass-transfer data revealed that the design of the gas separator is a very important factor affecting the mass-transfer rate. This has been already stated by Siegel and Merchuk (1991), based on data obtained in a split vessel ALR of rectangular cross section. The data and analysis presented here may lead to a generalized treatment of different kinds of ALRs. Research in this direction is in progress.

This work covers a rather low range of gas flow rates. More-

over, variables like the ratio of cross-sectional areas R, slenderness ratio S, surface tension, and gas diffusivity in the liquid have not been considered. Research efforts should be devoted to covering these variables to obtain a generally applicable equation for ALR design.

Acknowledgment

Data processing was performed with software kindly provided by Dr. Marc Siegel, Ben Gurion University of the Negev. The help of Mr. I Berzin in some of the computations is gratefully acknowledged. The authors are grateful to Professor Atkinson, Head of Biotechnology Div., CAMR, for his support and the provision of facilities. The assistance of the CID in setting the instrumentation and computer files handling is gratefully acknowledged.

Notation

A = free area for fluid flow, m^2
C = clearance, mm
C_e = response of the dissolved oxygen electrode, $kmol/m^3$
C_e^* = C_e in equilibrium with air
C_{eo} = initial value of C_e
D = internal diameter, m
D_L = diffusivity of the gas in the liquid, cm^2/s
g = gravitational constant, m/s^2
H = height of ungassed liquid, m
H_d = height of dispersion, m
J = superficial velocity based on the total cross section, m/s
K = consistency index, $N \cdot m^{-2} \cdot s^n$
K_B = frictional loss coefficient at the bottom
k_La = volumetric mass-transfer coefficient, s^{-1}
L = height, m
m = dimensionless mass-transfer coefficient (Eq. 8)
n = exponent in the power low rheological equation
P = pressure, Pa
t = time, s
T = temperature, °C
T_e = time constant of the oxygen electrode, s
v_∞ = free rise bubble velocity, m/s
V = volume, m^3
z = axial distance, m

Greek letters

γ = shear rate, s^{-1}
ϕ = holdup
Δ = difference
ρ = density, kg/m^3
σ = surface tension, $N \cdot m^{-1}$
μ = viscosity, $Pa \cdot s$
τ = shear stress, $N \cdot m^{-2}$

Subscripts

a = annulus
b = bottom
d = downcomer
dr = draft tube
eff = effective
fr = friction
G = gas
L = liquid
o = orifice
r = riser
s = separator
t = top
T = total

Dimensionless groups

DR = disengagement ratio
Eu' = modified Euler number, $\Delta P/\rho J_G^2$
Fr = Froude number, $J_G/\sqrt{(g\,D)}$
Ga = Galileo number, $g\,\rho_L^2 D^3/\mu^2$
M = bubble separation group, $D_s/4D$
R = diameter ratio, D/D_{dr}
S = slenderness ratio, L_{dr}/D
Sh = Sherwood number, $k_La\,D^2/D_L$
We_o = Weber number for the orifice, $V_o^2 d_o \rho_o/\sigma$
X_{dr} = bottom clearance ratio, C_b/D_{dr}
Y = top clearance ratio, C_t/D_{dr}

Literature Cited

Akita, K., T. Okazaki, and H. Koyama, "Gas Holdups and Friction Factors of Gas-Liquid Two-Phase Flow in Airlift and Bubble Column," *J. Chem. Eng. Japan*, **21**, 476 (1988).
André, G., C. W. Robinson, and M. Moo-Young, " ," *Chem. Eng. Sci.*, **38**, 1845 (1983).
APHA, *Standard Methods for the Examination of Water and Wastewater*, 15th ed., Amer. Health Assoc., Washington, DC (1981).
Bello, R. A., "A Characterization Study of Airlift Contactors for Applications to Fermentation," PhD Thesis, Univ. of Waterloo, Canada (1981).
Bello, R. A., C. W. Robinson, and M. Moo-Young, "Gas Holdup and Overall Oxygen Transfer Coefficient in Airlift Contactors," *Biotech. Bioeng.*, **27**, 369 (1985).
Bird, R. B., R. C. Armstrong, and O. Hassager, *Dynamics of Polymeric Liquids*, Wiley, New York (1987).
Blenke, H., "Loop Reactors," *Adv. in Biochem. Eng.*, **13**, 121 (1979).
Chakravarty, M., H. D. Singh, J. N. Baruah, and M. S. Iynegar, "Liquid Velocity in Gas-Lift Column," *Indian Chem. Eng.*, **16**, 17 (1974).
Chisti, M. Y., and M. Moo-Young, "Airlift Reactors: Characteristics, Applications and Design Considerations," *Chem. Eng. Commun.*, **60**, 195 (1987).
Chisti, M. Y., B. Halard, and M. Moo-Young, "Liquid Circulation in Airlift Reactors," *Chem. Eng. Sci.*, **43**, 451 (1988).
Chisti, M. Y., *Air Lift Bioreactors*, Elsevier, New York (1989).
Deng, X.-H., and Q. Li, "Investigation of Liquid Circulation and Gas Holdup in Airlift Loop Reactor," *Chem. Reaction Eng. and Technol.*, China, **2**, 48 (1986).
Fröhlich, S., M. Lotz, T. Korte, A. Lübbert, K. Schügerl, and M. Seekamp, "Characterization of a Pilot Plant Loop Bioreactor. I: Evaluation of the Phase Properties with Model Media," *Biotech. Bioeng.*, **38**, 43 (1991).
Garcia Calvo, E., "Fluid Dynamics of Airlift Reactors: Two Phase Friction Factors," *AIChE J.*, **38**, 1662 (1992).
Hwang, S. J., and L. S. Fan, "Some Design Considerations of a Draft Tube Gas-Liquid-Solid Spouted Bed," *The Chem. Eng. J.*, **33**, 49 (1986).
Joshi, J. B., V. V. Ranade, S. D. Gharat, and S. S. Lele, "Sparged Loop Reactors," *The Can. J. of Chem. Eng.*, **68**, 705 (1990).
Koide, K., K. Kurematsu, S. Iwamoto, Y. Iwata, and K. Horibe, "Gas Holdup and Volumetric Liquid-Phase Mass Transfer Coefficient in Bubble Column with Draught Tube and with Gas Dispersion into Annulus," *J. Chem. Eng. Japan*, **16**, 413 (1983).
Koide, K., S. Iwamoto, Y. Takasaka, S. Matsuura, E. Takahashi, M. Kimura, and H. Kubota, "Liquid Circulation, Gas Holdup and Pressure Drop in Bubble Column with Draught Tube," *J. Chem. Eng. Japan*, **17**, 611 (1984).
Koide, K., M. Kimura, H. Nitta, and H. J. Kawabata, "Liquid Circulation in Bubble Column with Draught Tube," *J. Chem. Eng. Japan*, **21**, 393 (1988).
Ladwa, M., A. Cameron, M. Bulmer, A. Picket, and J. C. Merchuk, "Influence of Draft Tube Clearance on Pressure Drop and Gas Holdup in a 250 Liter Airlift Reactor," Int. Conf. on Bioreactor Fluid Dynamics, R. King, ed., Elsevier, London, p. 395 (1988).
Lee, V. C. H., L. A. Glasgow, L. E. Erikson, and S. A. Patel, "Liquid Circulation in Airlift Reactors," *Biotechnology Processes—Scale Up and Mixing*, C. S. Ho and J. Y. Oldshue, eds., AIChE, New York, p. 50 (1987).
Lockhart, R. W., and R. C. Martinelli, "Proposed Correlation of Data for Isothermal Two-Phase Two-Component Flow in Pipes," *Chem. Eng. Prog.*, **45**, 39 (1949).
McManamey, W. J., and D. A. J. Wase, "Relationship Between the

Volumetric Mass Transfer Coefficient and Gas Holdup in Airlift Fermenters," *Biotechnol. Bioeng.*, **28**, 1446 (1986).
Merchuk, J. C., Y. Stein, and R. I. Mateles, "Distribution Parameter Model of an Airlift Fermenter," *Biotechnol. Bioeng.*, **22**, 1189 (1980).
Merchuk, J. C., and Y. Stein, "Local Holdup and Liquid Velocity in Airlift Reactors," *AIChE J.*, **27**, 337 (1981).
Merchuk, J. C., "Hydrodynamics and Holdup in Air-Lift Reactors," *Encyclopedia of Fluid Mechanics*, N. P. Cheremisinoff, ed., Vol. 3, Chap. 49, Gulf Publishing, Houston (1986).
Merchuk, J. C., "Tower Reactor Models," *Biotechnology.*, Vol. 3, Chap. 3, K. Schügerl, ed., Springer (1990).
Merchuk, J. C., "Shear Effect in Suspended Cultures," *Adv. Biochem. Eng.*, **44**, 65 (1991).
Merchuk, J. C., G. Osemberg, M. Siegel, and M. Shacham, "A Method for Evaluation of Mass Transfer Coefficients in the Different Regions of Air Lift Reactors," *Chem. Eng. Sci.*, **47**, 3517 (1992).
Nishikawa, M., H. Kato, and K. Hashimoto, "Heat Transfer in Aerated Tower Filled with non-Newtonian Liquid," *Ind. Eng. Chem. Process Des. Dev.*, **16**, 133 (1977).
Popovic, M., and C. W. Robinson, "External Circulation-Loop Airlift Bioreactors: Study of the Liquid Circulating Velocity in Highly Viscous non-Newtonian Liquids," *Biotechnol. Bioeng.*, **32**, 301 (1988).
Popovic, M., and C. W. Robinson, "Mass Transfer Studies in External Loops Airlifts and a Bubble Column," *AIChE J.*, **35**, 393 (1989).
Oshinowo, T., and M. E. Charles, "Vertical Two-Phase Flow: 2. Holdup and Pressure Drop," *Can. J. Chem. Eng.*, **52**, 438 (1974).
Perry, J. H., *Chemical Engineering Handbook*, 4th ed., McGraw-Hill, New York (1963).
Philip, J., J. M. Proctor, K. Niranjan, and J. F. Davidson, "Gas Holdup and Liquid Circulation in Internal Loop Reactors Containing Highly Viscous Liquids," *Chem. Eng. Sci.*, **45**, 651 (1990).
Siegel, M., J. C. Merchuk, and K. Schügerl, "Gas Recirculation in Air-Lift Reactors," *AIChE J.*, **32**, 179 (1986).
Siegel, M. H., and J. C. Merchuk, "Mass Transfer in a Air Lift Reactors: Effects of Gas Recirculation," *Bioreactors and Biotransformations*, G. W. Moody and P. B. Baker, eds., Elsevier, London, p. 350 (1987).
Siegel, M., and J. C. Merchuk, "Mass Transfer in a Rectangular Air Lift Reactor: Effects of Geometry in Gas Recirculation," *Biotechnol. Bioeng.*, **32**, 1128 (1988).
Siegel, M., M. Hallaile, and J. C. Merchuk, "Air Lift Fermenters: Principles and Applications," *Advances in Biotechnological Processes*, A. Mizrahi, ed., Vol. 7, A. R. Liss, Inc., New York, p. 80 (1988).
Siegel, M., S. Ben-Zvi, and J. C. Merchuk, "Measurement and Interpretation of Mass Transfer Data in Air-Lift Bioreactors," *Proc. APBioChE*, Kuyngju, Korea, p. 449 (Apr. 22-25, 1990).
Siegel, M., and J. C. Merchuk, "Hydrodynamics in Rectangular Air-Lift Reactors: Scaleup and the Influence of Gas-Liquid Separator Design," *Can. J. of Chem. Eng.*, **69**, 465 (1991).
Sukan, S. S., and E. Vardar-Sukan, "Mixing Performance of Airlift Fermenters against Working Volume and Draft Tube Dimensions," *Bioprocess Eng.*, **3**, 33 (1987).
Thomas, H. N., and D. A. Janes, "Fluid Dynamic Considerations in Air Lift Bioreactors," AIChE Meeting, Miami (Nov., 1986).
Umeno, S., T. Kumagai, and Y. Kawase, "Hydrodynamics and Mass Transfer in Bubble Columns with Non-Newtonian Media," German-Japanese Symp. on Bubble Columns, Kyoto, Soc. of Chemical Engineers, Japan, p. 117 (1991).
Verlaan, P., J. Tramper, K. van't Riet, and K. Luyben, "A Hydrodynamic Model for an Airlift Loop Bioreactor with External Loop," *Chem. Eng. J.*, **33**, B43 (1986).
Weiland, P., and U. Onken, "Differences in the Behavior of Bubble Columns and Airlift Reactors," *Ger. Chem. Eng.*, **4**, 40 (1981).
Weiland, P., "Influence of Draft Tube Diameter on Operation Behavior of Airlift Loop Reactors," *Ger. Chem. Eng.*, **7**, 374 (1984).

Appendix: Effects of Viscosity on Holdup Measurement

If the frictional pressure drop per unit length of tube is written (Merchuk and Stein, 1981) as:

$$\Delta P_{fr} = 2\, C_{fm}\, \rho_L\, J_L^2 D^{-1} \tag{A1}$$

where

$$C_{fr} = 0.046\, Re^{-0.2} = 0.046 \left(\frac{\rho_L D}{1-\phi}\right)^{-0.2} \left(\frac{J_L}{\mu}\right)^{-0.2} \tag{A2}$$

then

$$\Delta P_{fr} = 0.092\, \rho_L^{0.8}\, D^{-1.2} (1-\phi)^{0.2} \mu^{0.2} J_L^{1.8} \tag{A3}$$

From Eq. A3 it follows that the pressure drop depends on J_L and μ. However, an increase in viscosity will lead to a decrease in liquid velocity, and this will tend to temper the influence of μ on the ΔP.

Take, for example, a tenfold rise in viscosity. Such a rise would increase the pressure drop by $10^{-0.2} = 1.58$. To cancel this effect, the liquid velocity would have to fall by $(1.58)^{1/1.8}$, which is approximately 30%. Decreases of this order in the liquid velocity have been reported (Fields et al., 1984; Philip et al., 1990).

But even if this counterbalancing effect is neglected, the frictional pressure drop can be disregarded in the experimental device used here. Take, for example, the riser $D = 0.21$ m, assuming operation with water ($\rho_L = 10^3$ kg/m^3). A typical value for J_L would be 0.25 m/s. From Eq. A2 it can be obtained that $C_{fm} = 0.0052$. With the given diameter and the total height of the riser, 3.27 m, the total frictional pressure drop is 10.14 Pa. The pressure drop measurement in the riser, for the given conditions, gives a hydrostatic head of the order of 280 mm H_2O, on approximately 2,700 Pa. Therefore,

$$\frac{\Delta P_{fr}}{\Delta P_{\text{hyd}}} = \frac{10.14}{2{,}700} = 3.7\ 10^{-3} \tag{A4}$$

A tenfold increase in viscosity would produce a maximum increase in ΔP of 60% (and less, considering the counterbalancing effect of the liquid velocity), and therefore the effect of the frictional pressure drop would still be negligible.

All the above refers to Newtonian fluids. This situation may change for the case of non-Newtonian fluids, where the viscosity is a function of the shear rate. But, for the case of power law fluids, where the viscosity decreases as the shear rate increases; since the shear rate reaches is maximal at the walls, it is to be expected that the pressure drop would be less than that corresponding to a Newtonian liquid of equal effective viscosity. Taking the case of laminar flow, let us compare the expressions of specific frictional pressure drop for a Newtonian liquid from Poiseuille's expression:

$$Q = \left(\frac{R \Delta P_N}{2\mu}\right) \frac{\pi R^3}{4} \tag{A5}$$

The corresponding equation for a power law fluid is (Bird et al., 1987):

$$Q = \left(\frac{R \Delta P_{nN}}{2K}\right)^{1/n} \frac{\pi R^3}{\left(3 + \frac{1}{n}\right)} \tag{A6}$$

Taking for both liquids the same flow rate Q, the same radius and $K = m$, we get:

$$\Delta P_{nN} = (\Delta P_N)^n \left(\frac{2K}{R}\right)^{(1-n)} \left(\frac{3}{4} + \frac{1}{4n}\right)^n \qquad \text{(A7)}$$

In the above expression, the last parenthesis is a very mild function of n. It contributes with 12% for $n = 0.1$. For our system the contribution is below 4% and may be disregarded.

The result is that the ratio of pressure drop (non-Newtonian liquid/Newtonian liquid) is independent of K and proportional to $R^{3(1-n)}$. The latter ratio will be larger than unity only for extreme values of R. For the case of turbulent flow, the pressure drop is calculated by a similar procedure (Eqs. A1 to A3), but using a generalized Reynolds number as recommended by Perry (1963). Again, the pressure drop is negligible.

Manuscript received Jan. 5, 1993, and revision received Aug. 24, 1993.

Errata

Correct Figure 4 (p. 795) of the article titled "Oxygen Permeation through Thin Mixed-Conducting Solid Oxide Membranes" by Y.-S. Lin, W. Wang, and J. Han (May 1994, p.786) is:

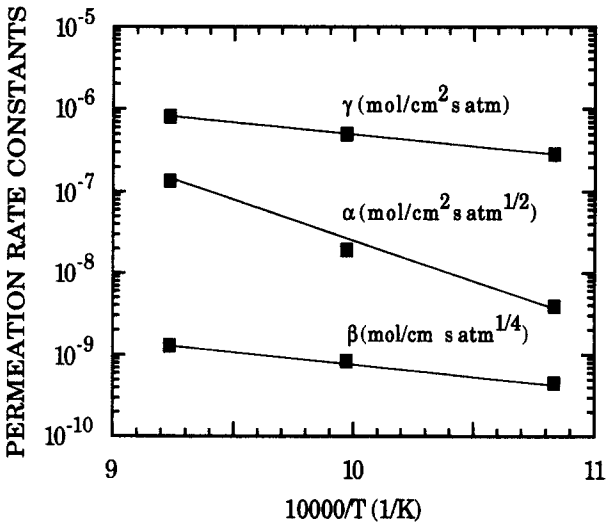

Figure 4. Arrhenius plots of permeation rate constants α, β and γ in the theoretical model for erbia stabilized bismuth oxide membrane.

In the article titled "Shape and Extent of the Void Formed by a Horizontal Jet in a Fluidized Bed" by Libin Chen and Herbert Weinstein (December 1993, p. 1901), the last conclusion should read "The jet penetration lengths measured agreed with the correlations of Zenz (1968), Merry (1971) and Shakhova (1968)," since correct calculations with the Zenz correlation were in good agreement with our data. In Figure 6, which compares our measured jet penetration lengths with correlations from the literature, the points from the Zenz (1968) correlation were not calculated correctly. Corrected Figure 6 is as follows:

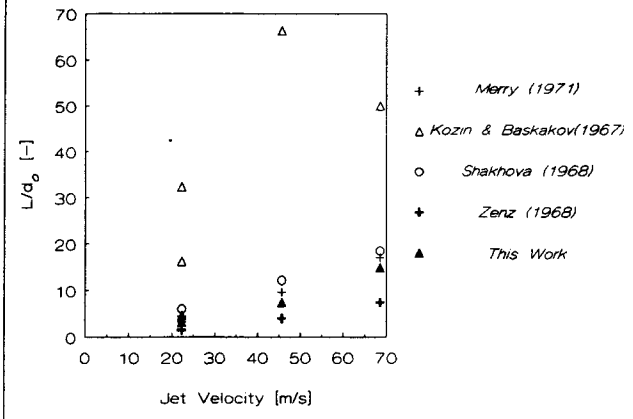

Figure 6. Comparison of experimental data for jet penetration length with predicted values.